Computational Materials Science 116 (2016) 96–102

Contents lists available at ScienceDirect

Computational Materials Science

journal homepage: www.elsevier.com/locate/commatsci

Numerical study of the surface hardening effect on the deformation-induced roughening in titanium polycrystals

Varvara Romanova [a,b,*], Ruslan Balokhonov [a,b], Olga Zinovieva [a], Valery Shakhidjanov [c]

[a] Institute of Strength Physics and Materials Science, The Russian Academy of Sciences, pr. Academicheskii 2/4, 634055 Tomsk, Russia
[b] National Research Tomsk Polytechnic University, pr. Lenina 30, 634050 Tomsk, Russia
[c] National Research Tomsk State University, pr. Lenina 36, 634050 Tomsk, Russia

ARTICLE INFO

Article history:
Received 27 May 2015
Received in revised form 15 September 2015
Accepted 17 September 2015
Available online 3 October 2015

Keywords:
Titanium alloys
Surface hardening
Deformation-induced roughening
Microstructure-based simulation
Crystal plasticity

ABSTRACT

A three-dimensional numerical analysis is performed of the deformation-induced roughening in polycrystalline specimens with and without surface-hardened layers. Three-dimensional microstructure-based constitutive models are developed, using crystal plasticity, and employed in finite element calculations of uniaxial tension. Grain structure is shown to be responsible for free surface roughening under uniaxial loading. Microscale stresses acting normally to the free surface in the bulk of the material are associated with normal displacements. The surface-hardened layer moves the grain structure away from the free surface, smoothing out the microscale folds formed due to displacements of individual grains, while the mesoscale surface undulations remain clearly visible.

1. Introduction

A great body of experimental and theoretical data (see, for example, [1–13]) indicates that plastic deformation is accompanied by the formation of a specific relief on an originally flat free surface. This phenomenon known as surface roughening is an undesirable feature deteriorating the surface reflectivity, wear resistance, and mechanical properties responsible for plastic strain localization under loading. Experimental investigations using scanning techniques have shown that the surface roughness exhibits a complex multiscale evolution pattern that goes far beyond the micro- and macroscopic phenomena involved [2]. This effect is evident as an orange peel pattern on the grain scale, roping, ridging, etc., on the mesoscale level, and a macroscopic waviness on the specimen length scale. Surface roughening is found to depend on many factors such as grain size, crystallographic texture, crystal lattice misorientation, strain hardening and loading conditions [1–13].

While ample experimental evidence has been gathered, the mechanisms involved and the factors responsible for the resulting roughening patterns are the subject of extended discussions among researchers. Further experimental and numerical investigations are required to elaborate efficient methods for suppressing the surface roughening mechanisms. As is shown in [9–12], surface modification by strain hardening or coating deposition techniques can effectively suppress roughening. The mechanisms lying behind this effect remain to be explored yet. Our goal here is to analyze this phenomenon numerically.

Apparently, multiscale roughening cannot be adequately described by a single model. Our study addresses micro- and mesoscale effects where grain structure plays an important role. A distinctive feature of the mesoscale surface roughening is that it is not individual grains but grain ensembles set in a cooperative motion to form folds, ridges and valleys, and hills and dimples on the material surface. While local microscale plastic deformation occurs by dislocation motion, cooperative processes appear to be of non-dislocation nature and cannot be described by dislocation theory alone. Construction of adequate models for deformation-induced surface roughening in the framework of the macroscopic mechanics presents difficulties as well, because no external forces act on the specimen free surface to give rise to out-of-plane surface displacements. Thus, the challenge is to examine roughening by means of microstructure-based models.

Recently, we have performed a numerical analysis of the surface roughening in polycrystalline steel, aluminum alloys, and coated homogeneous isotropic materials, using three-dimensional (3D)

* Corresponding author at: Institute of Strength Physics and Materials Science, The Russian Academy of Sciences, pr. Academicheskii 2/4, 634055 Tomsk, Russia. Tel.: +7 (3822) 286937; fax: +7 (3822) 492576.
E-mail address: varvara@ispms.tsc.ru (V. Romanova).

http://dx.doi.org/10.1016/j.commatsci.2015.09.045
0927-0256/

microstructure-based models [14–16]. The evolution of the surface roughness in a two-phase coated material with an irregular coating-substrate interface was calculated in [14]. Polycrystalline steel and aluminum alloys were studied numerically in [15,16]. The effects of the grain shape and boundary conditions on the qualitative and quantitative characteristics of the surface roughness were illustrated using two representative microstructures with extended and equiaxial grains as an example [16]. The computational results obtained lead us to conclude that the coating-substrate interface and the grain boundaries lying within the subsurface layer are responsible for the formation of the surface relief under loading.

Continuing the investigations along these lines, we performed numerical simulations of the surface roughening in surface-modified polycrystalline titanium subjected to uniaxial tension. The constitutive response of polycrystalline grains is described with the use of crystal plasticity theory.

2. Computational models

2.1. Three-dimensional microstructures

To investigate the mechanical aspects of micro- and mesoscale surface roughening, numerical simulations were performed by means of 3D models taking an explicit account of polycrystalline structure. Three-dimensional microstructural models of polycrystalline titanium with and without a surface-hardened layer were built by a step-by-step packing (SSP) method proposed in [17] and modified in [15] to obtain periodic microstructures. To generate a polycrystalline model, all grains are grown at the same rate on a regular mesh in accordance with a spherical law until the entire computational volume is filled without gaps or overlaps. Thus, we have generated a 3D polycrystal consisting of 1600 grains on a regular cubic $200 \times 75 \times 200$ mesh with the element size being $10 \times 10 \times 10$ μm (Fig. 1a). The size of the polycrystalline model is $2000 \times 750 \times 2000$ μm along X_1, X_2 and X_3 axes, respectively (an average grain size is 120 μm). To design a surface-hardened polycrystal, a structureless layer has been generated on the surface of the base material (Fig. 1b). The hardened layer thickness is 80 μm (8 elements).

2.2. Constitutive response of grains

The constitutive response of grains is described by Hooke's law expressed in the rate form as

$$\dot{\sigma}_{ij} = C_{ijkl}\dot{\varepsilon}^e_{kl} \tag{1}$$

where σ_{ij} and ε^e_{ij} are the stress and elastic strain tensors and C_{ijkl} is the tensor of elastic moduli. Here and henceforward, the upper dot denotes the time derivative. Due to the symmetry of a hexagonal lattice, titanium single crystals are characterized by twelve non-zero elastic moduli, five of them being independent: $C_{1111}, C_{1122}, C_{1133}, C_{3333}$, and C_{2323}. Let us introduce a Cartesian coordinate system so that two coordinate axes coincide with the crystallographic axes and the third one lies on a basal plane. Then, the stress tensor components in the local coordinate system are calculated in the following way:

$$\begin{aligned}
\dot{\sigma}_{11} &= C_{1111}\dot{\varepsilon}^e_{11} + C_{1122}\dot{\varepsilon}^e_{22} + C_{1133}\dot{\varepsilon}^e_{33}\\
\dot{\sigma}_{22} &= C_{1122}\dot{\varepsilon}^e_{11} + C_{1111}\dot{\varepsilon}^e_{22} + C_{1133}\dot{\varepsilon}^e_{33}\\
\dot{\sigma}_{33} &= C_{1133}\left(\dot{\varepsilon}^e_{11} + \dot{\varepsilon}^e_{22}\right) + C_{3333}\dot{\varepsilon}^e_{33}\\
\dot{\sigma}_{12} &= (C_{1111} - C_{1122})\dot{\varepsilon}^e_{12}\\
\dot{\sigma}_{13} &= 2C_{2323}\dot{\varepsilon}^e_{13}\\
\dot{\sigma}_{23} &= 2C_{2323}\dot{\varepsilon}^e_{23}
\end{aligned} \tag{2}$$

Using the total strain rate tensor ε_{ij} expressed as the sum of an elastic and a plastic part

$$\varepsilon_{ij} = \varepsilon^e_{ij} + \varepsilon^p_{ij} \tag{3}$$

gives

$$\dot{\sigma}_{ij} = C_{ijkl}\left(\dot{\varepsilon}_{kl} - \dot{\varepsilon}^p_{kl}\right). \tag{4}$$

It is common practice to describe the behavior of polycrystal plastic deformation with the use of crystal plasticity models taking an explicit account of the crystallographic orientations of individual grains [13,18–20]. Following this approach, we consider a polycrystalline specimen as an aggregate of single crystals with different crystallographic orientations relative to a global coordinate system plotted in Fig. 1. The plastic strain rate tensor expressed in terms of crystal plasticity is of the form

$$\dot{\varepsilon}^p_{ij} = \frac{1}{2}\sum_{\alpha}\dot{\gamma}^{(\alpha)}\left(s^{(\alpha)}_i m^{(\alpha)}_j + s^{(\alpha)}_j m^{(\alpha)}_i\right), \tag{5}$$

where $s^{(\alpha)}_i$ and $m^{(\alpha)}_i$ are the slip direction and slip plane normal vectors for a slip system α. For quasi-static loading at room temperature, it is reasonable to define the shear strain rate $\dot{\gamma}^{(\alpha)}$ through the dependence on the Schmid resolved shear stress $\tau^{(\alpha)}$ calculated for each slip system:

$$\tau^{(\alpha)} = s^{(\alpha)}_i \sigma_{ij} m^{(\alpha)}_j. \tag{6}$$

In the framework of the viscoplastic approach [20], $\dot{\gamma}^{(\alpha)}$ is approximated by a power law, using the following relation [21]:

$$\dot{\gamma}^{(\alpha)} = \dot{\gamma}_0 \left|\frac{\tau^{(\alpha)}}{\tau^{(\alpha)}_{SR}}\right|^{\nu} sign(\tau^{(\alpha)}), \tag{7}$$

where $\dot{\gamma}_0$ is the reference slip rate and ν is the strain rate sensitivity coefficient. These coefficients were chosen to describe the strain-

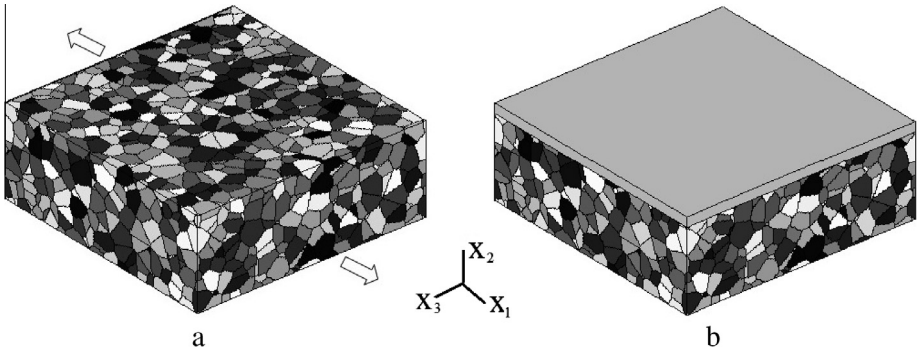

Fig. 1. Polycrystalline models without (a) and with a hardened layer (b).